Phase transformation reactions in rapidly solidified Al-6.5Fe-1.5V alloys

R. TONGSRI, E. J. MINAY, R. P. THACKRAY, R. J. DASHWOOD, H. B. MCSHANE
Department of Materials, Imperial College of Science, Technology and Medicine, Prince Consort Road, London SW7 2BP, UK

Phase transformation reactions, occurring during heating of as-atomised Al-6.5Fe-1.5V powders, extrusion of the powders, and heating of the as-extruded alloys produced from the powders, have been studied by DSC, XRD and TEM. The DSC studies of the as-atomised powders revealed several phase transformation reactions. The solid solution in zone A decomposed to form metastable phases at 360°C. These metastable phases further transformed to form equilibrium phases at 500°C. The microquasi-crystalline icosahedral (MI) phase particles present in zone A and zone B transformed to equilibrium phases at 500°C. The globular clusters of microquasi-crystalline icosahedral (GCMI) phase particles in zone C transformed polymorphously to icosahedral (I) phase particles at 450°C. These reactions were believed to occur during extrusion of the powders. During heating of the as-extruded alloys produced from coarse powder particles, I phase transformed polymorphously to hexagonal phase at 550°C. The hexagonal phase decomposed to monoclinic $Al_{45}(V, Fe)_7$ and $Al_{13}Fe_4$ phases upon heating for longer times. © *2001 Kluwer Academic Publishers*

1. Introduction

There has been growing interest in the development of rapidly solidified Al-Fe based alloys that are potential candidates for elevated temperature applications. The ability of materials to retain their mechanical properties at elevated temperatures is attributed to the thermal stability of the microstructures. The thermal stability of the microstructures is controlled by both the activation energy for diffusion and the solubility of the solute or alloying elements in the solid state. It is well known that microstructure is closely related to the mechanical properties of materials. An investigation of the phase transformation reactions occurring during the processing of these materials at elevated temperatures would provide basic understanding of the thermal stability of the microstructures and the performance of the materials. Rapidly solidified Al-Fe-V alloys have been shown to be promising candidates amongst several rapidly solidified Al-Fe-X alloys [1–3]. Investigations into melt-spun Al-Fe-V alloys [4, 5] have been concerned only with the stability of the icosahedral (I) phase as a function of alloy composition. Phase transformation reactions of some other phases in these alloys have not been fully investigated. Although precipitation reactions occurring during heating of as-cast alloys in the form of powder or melt-spun ribbons have been investigated [6–8], these investigations have provided only limited information for phase transformation reactions of some intermetallic phases. In this paper, microstructures of as-atomised powders, as-extruded alloys and heat-treated products have been investigated in order to deduce the phase transformation reactions,

which possibly occur during processing of rapidly solidified Al-6.5Fe-1.5V alloy at elevated temperatures. Phase identification was carried out using characterization techniques such as XRD, TEM and EDS. To ascertain phase identification, some known phases which appear in the literature [9–16] were used to compare with the phases observed in this study.

2. Experimental

The as-atomised powders, gas classified into size fractions, were received from ALPOCO, UK. Each powder size fraction was uniaxially cold-compacted to form a billet. The billet was preheated to 500°C and extruded to a rod-shaped product at an extrusion ratio of 18 : 1. Differential scanning calorimetry (DSC) was employed to study phase transformation reactions in all powder size fractions. For investigation of phase transformation reactions during heat-treatment of the as-extruded alloys, the rods were heat-treated at 500–550°C for different times. Phase identification in the as-atomised powders, as-extruded alloys, and heat-treated products was carried out using X-ray diffraction (XRD), and transmission electron microscopy (TEM) equipped with energy dispersive X-ray microanalysis spectrometry (EDS). TEM specimens of the as-atomised powders were prepared by electrochemical deposition of nickel onto the powders on the surface of a cathode. The resulting nickel foils, impregnated with powder, were ground and punched into 3 mm diameter discs. The discs were jet-electropolished using 10 volume % of perchloric acid in ethanol at 65 V and −45°C. TEM specimens

of the solid samples (the as-extruded alloys and the heat-treated products) were prepared by the standard method. The discs were jet-electropolished using 30 volume % of perchloric acid in methanol at 20 V and $-30\,°C$.

3. Results and discussion

3.1. Microstructures of the as-atomised powders

Fine powder particles ($\leq 5\ \mu$m) exhibited two types of microstructure (Fig. 1a). The first, designated as zone A, consists of fine particles randomly distributed in the α-Al matrix resulting from planar front solidification. The second, designated as zone B, consists of fine particles entrapped in the intercellular regions of microcellular structures. The fine particles in zone A and zone B exhibited selected area electron diffraction patterns (SADPs) with ring patterns (Fig. 1a) and Fig. 2b). The d-spacing values of the diffraction rings were consistent to those of the icosahedral Al_4Mn (I-Al_4Mn) phase [9]. Due to their d-spacing values, fine particles in zone A and zone B are believed to be micro-quasicrystalline icosahedral (MI) phase particles. A microstructure consisting of very fine and uniformly distributed particles in an α-Al matrix (similar to zone A) was observed in a melt-spun Al-Fe-Mo-V alloy [10]. These particles were identified to be the MI phase using a convergent beam electron diffraction (CBED) technique. The intercellular phases in rapidly solidified Al-Fe [11], and Al-Fe-Si [12] alloys also exhibited ring diffraction patterns, corresponding to the presence of MI phase in the intercellular regions.

In powder particles with diameters of 5–15 μm, microstructures consisted of zone B as the main morphology. This type of morphology was also observed in melt spun Al-Fe-V alloys [1, 2]. Some globular particles are evident at the powder particle rim, opposite to the nucleation site, N (Fig. 1b).

Microstructures of powder particles larger than 15 μm consisted of globular particles entrapped in coarse cells (Fig. 1c). SADPs exhibited a ring pattern from such globular particles (Fig. 2a). The d-spacing values corresponding to the SADP were found to be consistent with those of the I-Al_4Mn phase [9]. This indicates that the globular particles are globular clusters of MI (GCMI) phase particles. EDS analyses performed

on several GCMI particles showed that their composition was Al_x(Fe, V) where $x = 5$ to 6. The GCMI phase is therefore designated as GCMI-Al_x(Fe, V). The d-spacing values of the GCMI-Al_x(Fe, V) and the intercellular phases, compared to those of the I-Al_4Mn phase, are given in Table I.

XRD of the as-atomised powder (Fig. 3) confirmed the presence of Al_6Fe and the phases constructed with icosahedral units (PCI). Note that the term PCI includes MI, GCMI, I, and some quasi-crystalline approximants with structures constructed with icosahedral units.

The term D[v, 0.5] μm is known as the volume median diameter, and is the value for which 50 percent of the particles measured are less than the stated size.

3.2. Phase transformation reactions in the as-atomised powders

DSC (Fig. 4) showed a variation of exotherms amongst the powder size fractions. These DSC scans were carried out within the temperature range of 25° to 600°C at a rate of 10 °C/min. Because DSC exotherms were broad and the onset temperatures were difficult to determine, the peak temperature was therefore chosen to represent each exotherm. The observed exotherms designated as A, B, and C corresponded to peak temperatures of 360°C, 500°C and 450°C, respectively.

Exotherm A was observed only for powder size fractions of fine powder particles, in which zone A was the predominant microstructure. This suggests that the exotherm A may correspond to a phase transformation reaction occurring in zone A, such as decomposition of the α-Al solid solution to form Al_6Fe phase. Such precipitation of Al_6Fe phase has been reported to occur during annealing of splat-cooled Al-Fe alloy in the temperature range of 300°C to 470°C [13].

The exotherm B was observed in all powder size fractions. To ascertain the reactions involved, a powder size fraction of fine powder particles was heat-treated at 500°C for up to 30 minutes. The intermetallic phases in the heat-treated powder particles were characterised using TEM and XRD. The microstructure of such a heat-treated powder particle (Fig. 5) clearly exhibited needle-like particles. Phase identification using XRD (Table II) showed the possible presence of

TABLE I The measured d-spacing values, relative intensities and indexing of GCMI-Al_x(Fe, V) and intercellular phase in Al-6.5Fe-1.5V powder particles, compared to those of I-Al_4Mn phase

Ring number	GCMI-Al_x(Fe, V)		Intercellular phase		I-Al_4Mn		
	d-value (nm)	Int.	d-value (nm)	Int.	d-value (nm)	Int.	Indexing
R1	0.385	m	0.385	d	0.3850	22	110001
R2	0.218	vs	0.218	vs	0.2170	100	100000
R3	0.207	vs	0.207	vs	0.2065	78	110000
R4	0.151	w	0.151	w + d	0.1496	11	111000
R5	0.127	w	0.127	w + d	0.1275	20	101000
R6	0.109	w	0.109	w + d	0.1085	7	200000

Note: w = weak, m = medium, s = strong, vs = very strong, and d = diffused.
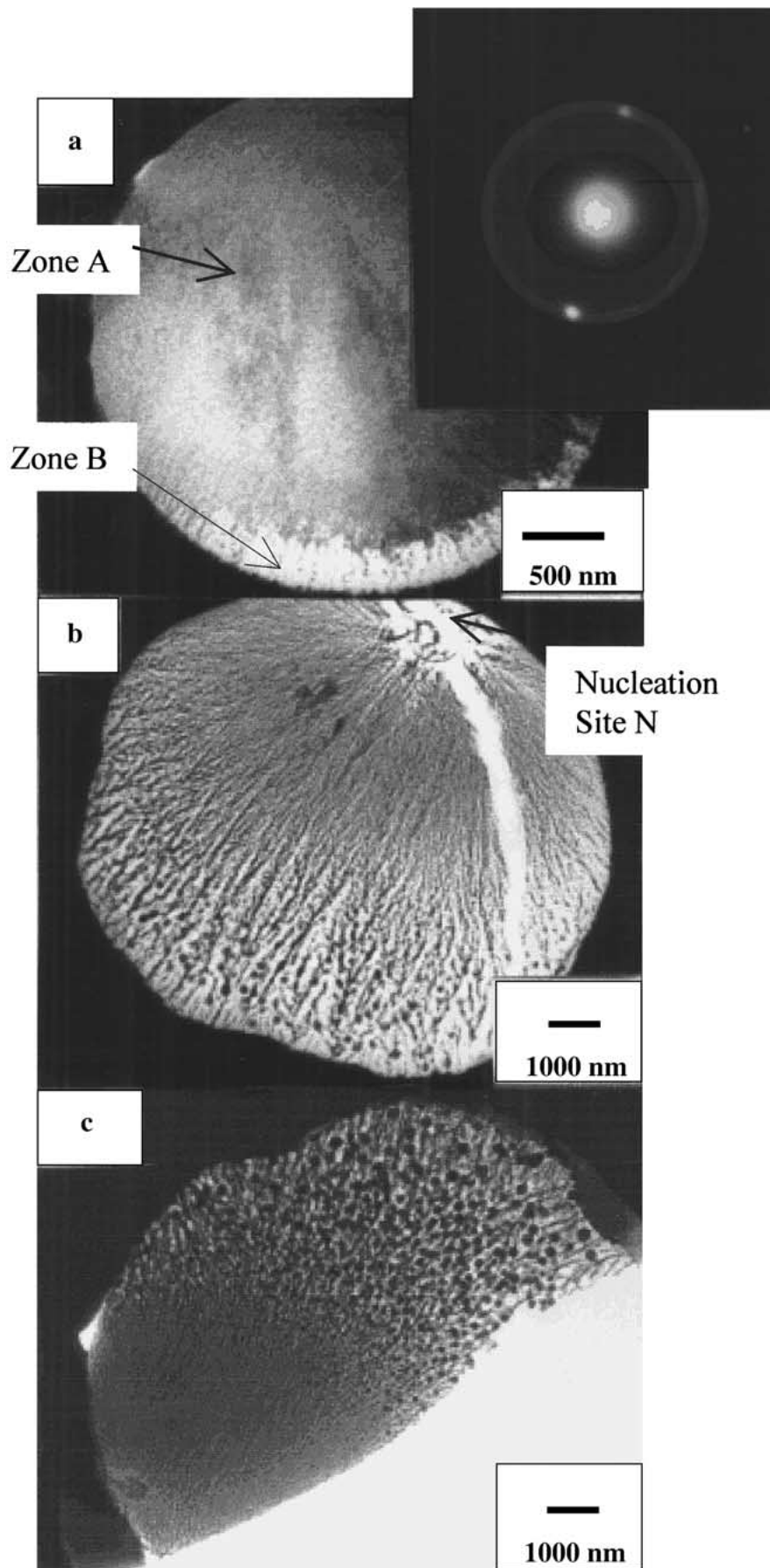
Figure 1 Bright field TEM images of the as-atomised Al-6.5Fe-1.5V powders of size (a) <5 μm, (b) 5–15 μm, (c) >15 μm.
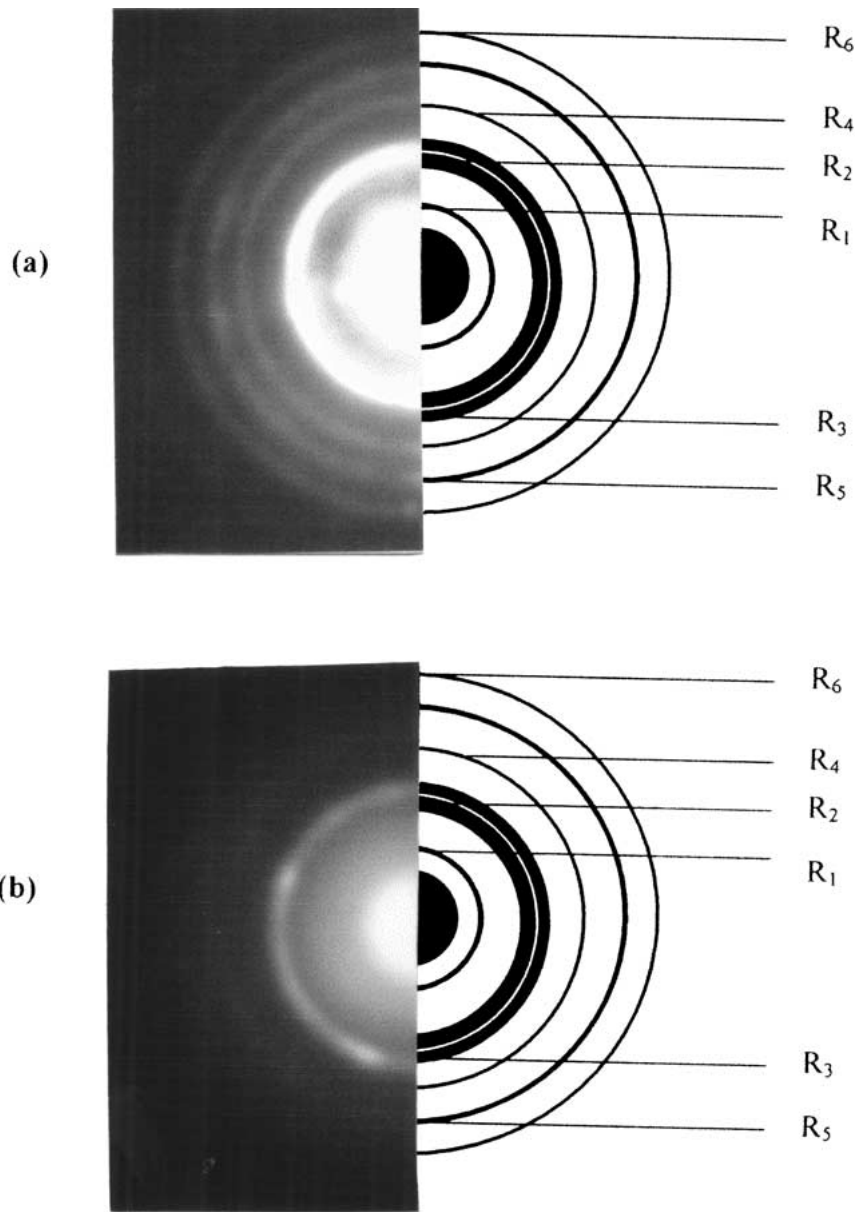
Figure 2 SADPs of (a) GCMI-Al$_x$(Fe, V) phase in a larger sized powder particle, and (b) intercellular phase, in a smaller sized powder particle.

TABLE II Phase identification in heat-treated (500–600°C for up to 72 hours) Al-6.5Fe-1.5V powders D[v, 0.5] = 50 μm using XRD

d-value, $\alpha 1$ (nm)	Relative Intensity	Phase
0.394	1.2	Al$_{13}$Fe$_4$
0.350	0.7	Al$_{13}$Fe$_4$
0.333	0.6	Al$_{13}$Fe$_4$
0.215	1.8	Al$_{13}$Fe$_4$ + Al$_{45}$(V, Fe)$_7$
0.209	4.0	Al$_{13}$Fe$_4$ + Al$_{45}$(V, Fe)$_7$
0.206	4.3	Al$_{13}$Fe$_4$ + Al$_{45}$(V, Fe)$_7$

Figure 3 XRD patterns of different size fractions, D[v, 0.5], of as-atomised Al-6.5Fe-1.5V powder.

Al$_{13}$Fe$_4$ and Al$_{45}$(V, Fe)$_7$. Although this data does not definitively prove the presence of Al$_{45}$(V, Fe)$_7$, the most likely reactions corresponding to exotherm B were therefore attributed to the formation of Al$_{13}$Fe$_4$ and Al$_{45}$(V, Fe)$_7$.

DTA exotherms with peak temperatures of 444°C for rapidly solidified Al-8 wt. % Fe, and of 495°C for rapidly solidified Al-10 wt. % Fe-2 wt. % V, have been attributed to precipitation of θ'Al$_3$Fe [6]. The precipi-
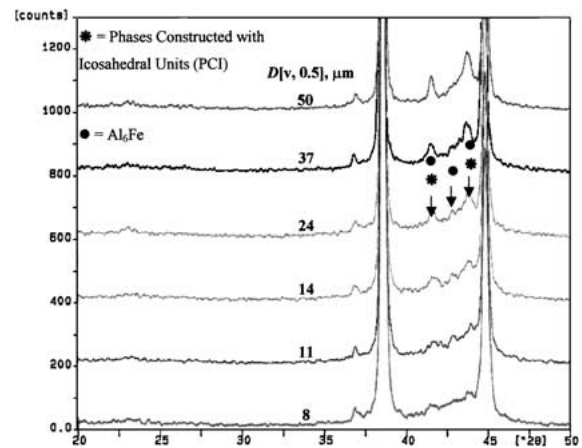
tation of equilibrium θ Al$_3$Fe was suggested to occur at 595°C in Al-8 wt. % Fe. However, DTA study of melt-spun Al$_{86}$Fe$_{14}$ alloy has shown that the reaction giving rise to an exotherm at 527–577°C corresponds to the
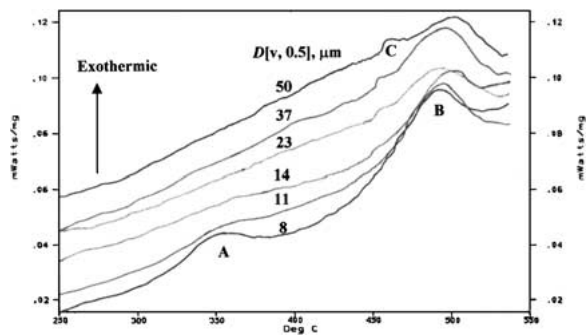
Figure 4 DSC scans from different size fractions of as-atomised Al-6.5Fe-1.5V powder.

transition Al_6Fe to Al_3Fe [7]. The DSC exotherm temperature corresponding to the same reaction was 450°C in melt-spun Al-8 wt. % Fe [8].

The exotherm C was found to relate to GCMI-$Al_x(Fe, V)$ particles in zone C. The magnitude of the exotherm C increased with increasing size and volume fraction of GCMI-$Al_x(Fe, V)$ particles. Microstructures of the as-extruded alloys produced from coarse powder particles included globular particles exhibiting SADPs, characteristic of I phase. These globular particles were identified as I-$Al_x(Fe, V)$ (§ 3). This suggests that the reaction corresponding to exotherm C is transformation from GCMI-$Al_x(Fe, V)$ to I-$Al_x(Fe, V)$. Since the compositions of both phases are the same but their structures are different, this phase transformation can be classified as polymorphous.

3.3. Microstructures of the as-extruded alloys

The microstructures of the as-extruded alloys varied with powder particle size fraction. Powder size fractions with $D[v, 0.5] \leq 14\ \mu m$, exhibited extruded microstructures that featured fine intermetallic particles

(Fig. 6a). These particles were observed to decorate grain boundaries and/or were present inside the grains. Powder size fractions with $D[v, 0.5] > 14\ \mu m$ in contrast gave typically banded structures, consisting of areas containing fine intermetallics and areas containing globular particles. A bright field TEM image of this banded structure is shown in Fig. 6b.

XRD (Fig. 7) indicated the presence of Al_6Fe, $Al_{13}Fe_4$, $Al_{45}(Fe, V)_7$ and PCI. TEM also revealed these phases plus a few unidentified particles. The PCI phase was found in the form of globular particles, which were I phase. No other quasi-crystalline phases were observed in the as-extruded alloys. SADPs of a globular I phase particle are shown in Fig. 8. EDS analyses performed on several globular icosahedral particles showed that their composition was $Al_x(Fe, V)$, where $x = 5$ to 6. The globular icosahedral phase is thus designated here as I-$Al_x(Fe, V)$.

3.4. Heat-treatment of the as-extruded alloys

The as-extruded alloys produced from coarse powder particle size fractions were chosen for investigation of phase transformation reactions during heat-treatment. Heat treatments were carried out between 500 and 550°C for different times. During heat-treatment, metastable phases, such as I-$Al_x(Fe, V)$ and Al_6Fe, were observed to transform to metastable and/or equilibrium phases. Equilibrium phases, such as $Al_{13}Fe_4$ and $Al_{45}(Fe, V)_7$, coarsened dramatically in this temperature range. It is well known that Al_6Fe transforms to $Al_{13}Fe_4$ at high temperatures. I-$Al_x(Fe, V)$ phase transformed to H-$Al_x(Fe, V)$ phase [14] during the heating of the as-extruded alloy at temperatures of $\geq 500\,°C$. The H-$Al_x(Fe, V)$ phase decomposed to equilibrium phases upon further heating. This staged decomposition of the I-$Al_x(Fe, V)$ phase may also correspond to the exotherm B of the DSC curves. Details of this reaction series observed during heat-treatment of the
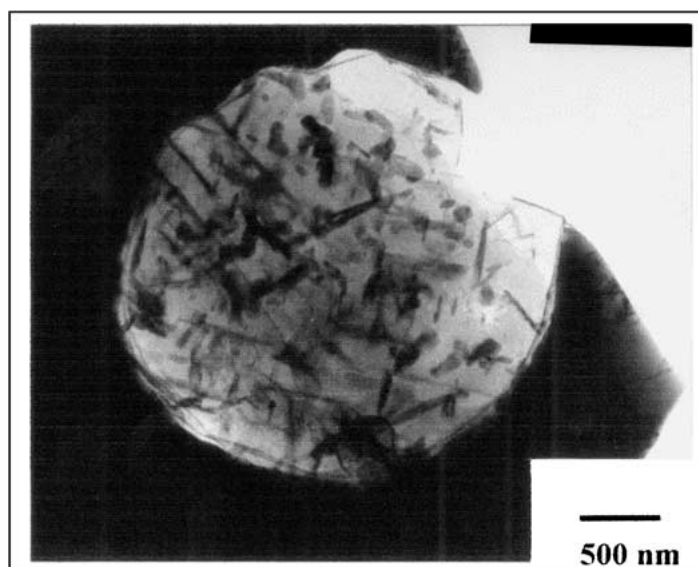

Figure 5 Bright field TEM image of an Al-6.5Fe-1.5V powder particle heat treated at 500°C for 10 minutes.
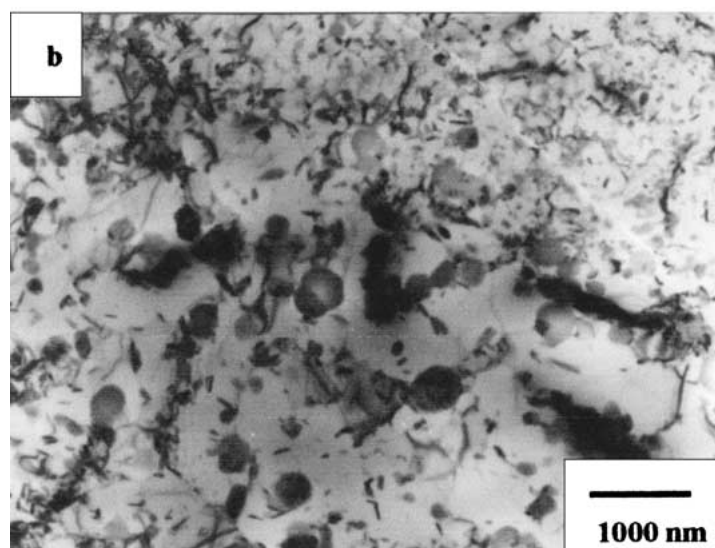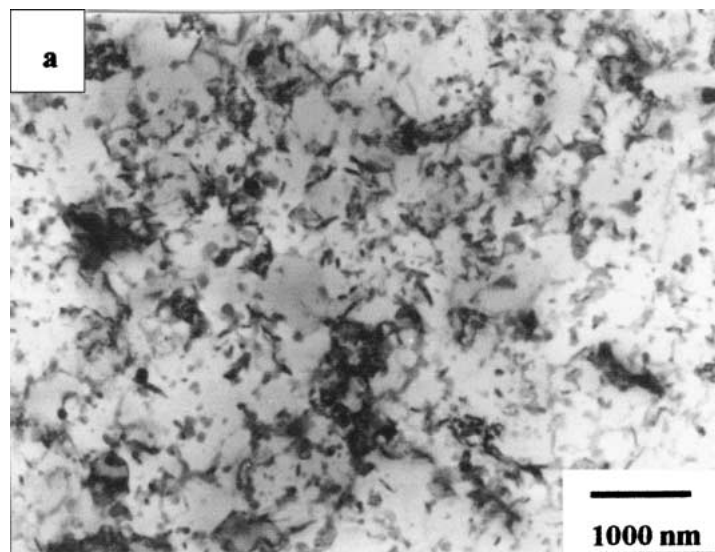
Figure 6 Microstructures of the as-extruded alloys produced from powder size fractions: (a) with $D[v, 0.5] \leq 14$ μm, (b) with $D[v, 0.5] > 14$ μm.

as-extruded alloys containing I-Al$_x$(Fe, V) phase are given below.

3.4.1. Transformation from I-Al$_x$(Fe, V) to H-Al$_x$(Fe, V)

The I-Al$_x$(Fe, V) phase was observed to be stable for up to 30 minutes during heat-treatment at 550°C. With further heating, the I-Al$_x$(Fe, V) phase transformed to globular crystalline phase. EDS analyses performed on several such globular crystalline particles showed that their composition was the same as I-Al$_x$(Fe, V). SADPs of the globular crystalline phase as shown in Fig. 9 indicated that this was a hexagonal phase. This phase was thus designated as H-Al$_x$(Fe, V). Since the
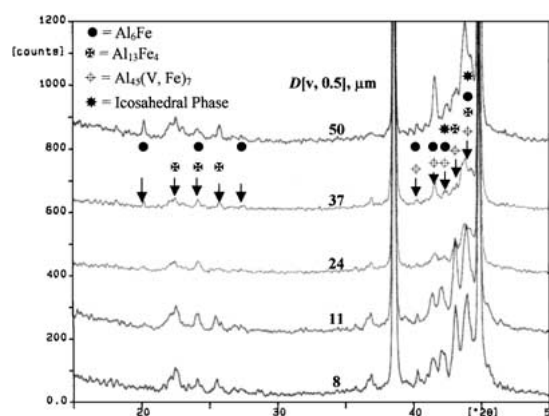

Figure 7 XRD patterns of the as-extruded Al-6.5Fe-1.5V alloys produced from different powder particle size fractions.
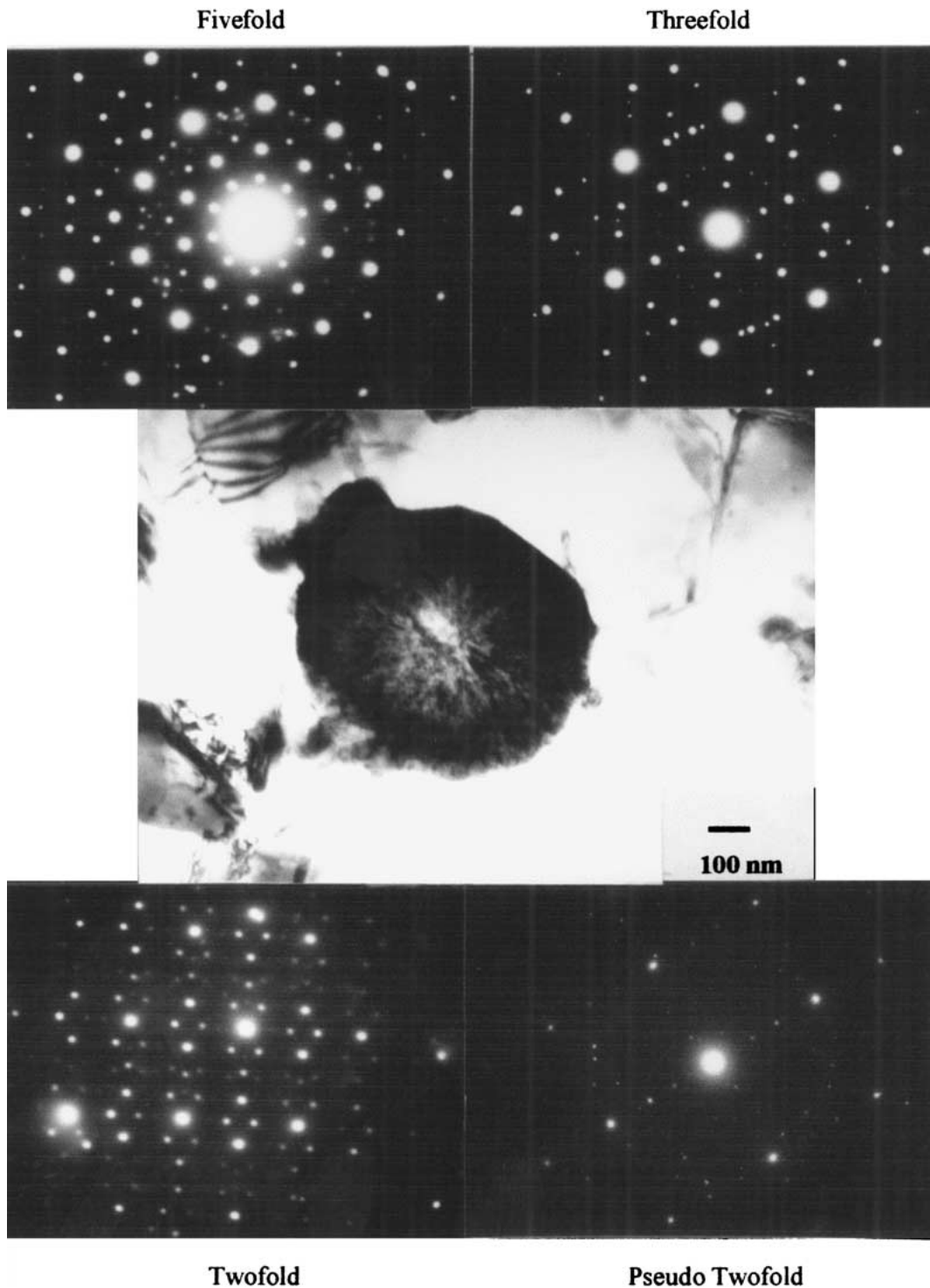
3202

Figure 8 Bright field TEM image and electron diffraction patterns of I-Al$_x$(Fe, V).

particle shape and composition of I-Al$_x$(Fe, V) and H-Al$_x$(Fe, V) phases are the same, but their crystal structures are different, it is possible that this phase transformation occurs polymorphously.

SADPs of H-Al$_x$(Fe, V) phase were observed to be identical to those of the hexagonal phase found in strip-cast and spray-cast Al-Fe-V-Si alloys [14], and were also similar to those of hexagonal Al$_6$Cr$_{0.5}$Ni$_{0.5}$ [15], and μ-Al$_4$Cr [16] phases. The Al$_6$Cr$_{0.5}$Ni$_{0.5}$ phase is structurally related to the decagonal phase, whereas

μ-Al$_4$Cr is structurally related to both icosahedral and decagonal phases.

3.4.2. Transformation from H-Al$_x$(Fe, V) to Al$_{13}$Fe$_4$ and Al$_{45}$(V, Fe)$_7$

With further heating at 550°C for up to 48 hours, the microstructures of the heat-treated products consisted of plate-like Al$_{13}$Fe$_4$ particles. In some areas, the Al$_{13}$Fe$_4$ was observed to exist next to knife
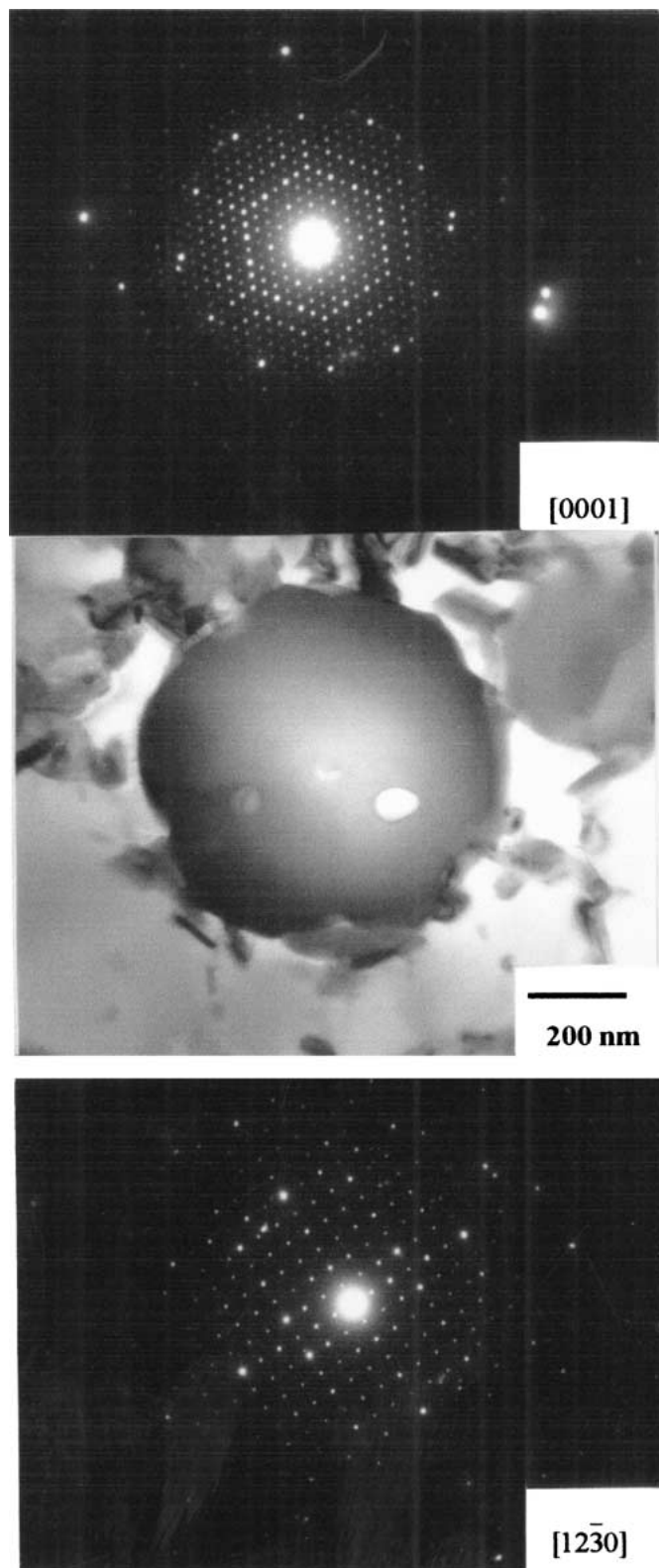
3203

Figure 9 Bright field TEM image and electron diffraction patterns of H-Al$_x$(Fe, V) after a heat treatment at 550°C for longer than 30 minutes.

blade-shaped particles (Fig. 10). The composition of the knife blade-shaped particle as determined by EDS was found to be Al$_{45}$(V, Fe)$_7$. Indexing of SADPs of Al$_{45}$(V, Fe)$_7$ phase using lattice parameters of the monoclinic Al$_{45}$V$_7$ phase was successful. This indicates that the Al$_{45}$(V, Fe)$_7$ phase is isostructural with the Al$_{45}$V$_7$

phase. The juxtaposition of Al$_{13}$Fe$_4$ and Al$_{45}$(V, Fe)$_7$ particles may indicate that these two phases result from decomposition of the crystalline Al-Fe-V phases which can be either unidentified Al-Fe-V or H-Al$_x$(Fe, V) phases. SADPs of Al$_{13}$Fe$_4$ and Al$_{45}$(V, Fe)$_7$ are shown in Fig. 10.

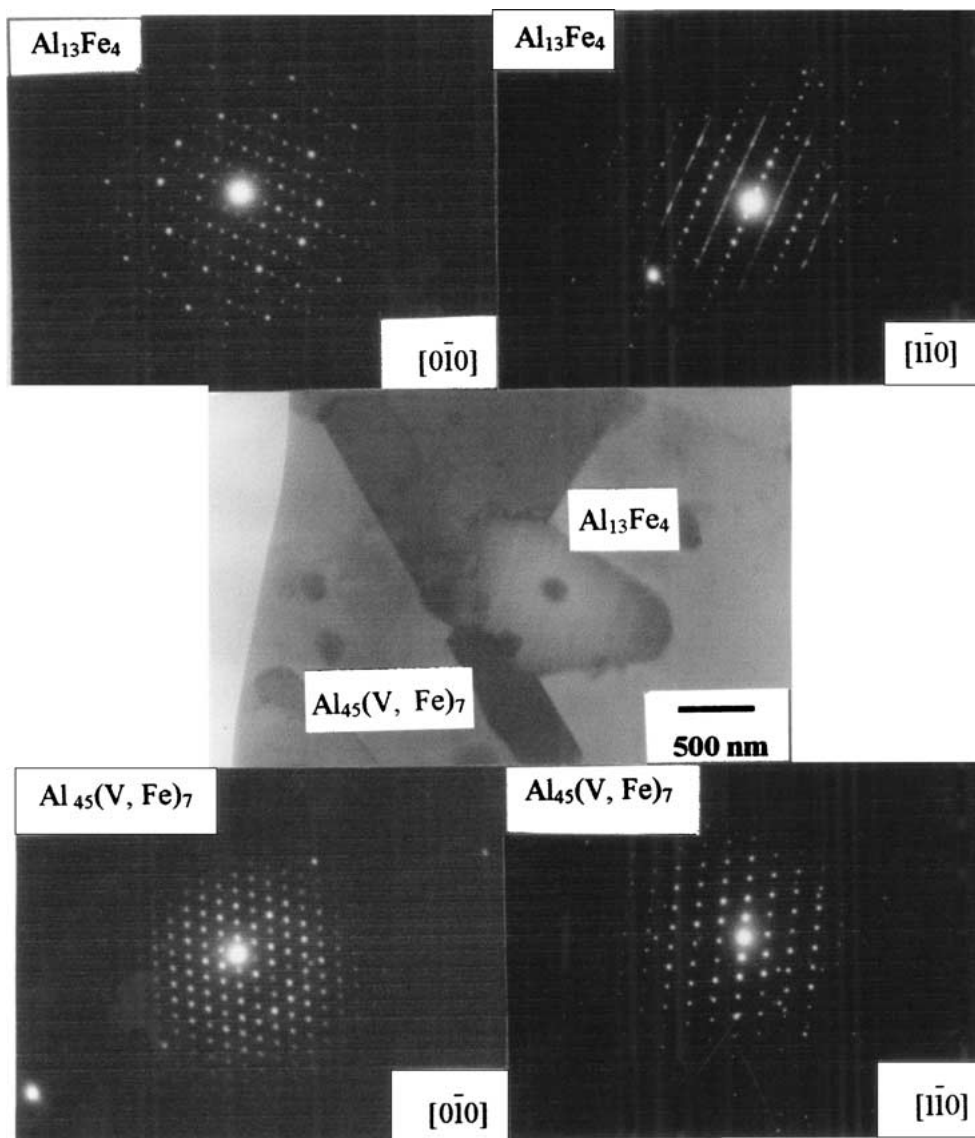*Figure 10* Bright field TEM image showing $Al_{13}Fe_4$ and Al_{45} (V, Fe)$_7$ and their electron diffraction patterns after a heat treatment at 550°C for 48 hours.

4. Conclusions

Several phase transformation reactions occur during the heating of as-atomised Al-6.5Fe-1.5V powders depending on the powder size fraction investigated. In fine powder particles, the supersaturated solid solution in zone A decomposes at 360°C to form metastable phases, which then decompose to form equilibrium phases at 500°C. The MI phase particles in zone A and zone B also decompose to form equilibrium phases at 500°C. The GCMI-Al_x(Fe, V) phase transforms to the more ordered I-Al_x(Fe, V) phase at 450°C.

The reactions mentioned above should occur during hot extrusion of the as-atomised powders. The phases, resulting from those reactions, remain in the microstructures of the as-extruded alloys. These phases include $Al_{13}Fe_4$, Al_{45}(V, Fe)$_7$, Al_6Fe, I-Al_x(Fe, V), and unidentified Al-Fe-V phases.

During heat-treatment of the as-extruded alloys, the I-Al_x(Fe, V) phase transforms to the H-Al_x(Fe, V) phase. The latter phase decomposes to form $Al_{13}Fe_4$ and Al_{45}(V, Fe)$_7$ phases upon further heating.

References

1. D. J. SKINNER and K. OKAZAKI, *Scripta Metall.* **18** (1984) 905.
2. D. J. SKINNER, K. OKAZAKI and C. M. ADAM, in "Rapidly Solidified Powder Aluminum Alloys," edited by M. E. Fine and E. A. Starke (American Society for Testing and Materials, Philadelphia, 1986) p. 211.
3. R. J. DASHWOOD, Report, BRITE EURAM, BREU-0356-C (1993).
4. D. J. SKINNER, V. R. V. RAMANAN, M. S. ZEDALIS and N. J. KIM, *Mater. Sci. Eng.* **99** (1988) 407.
5. M. S. ZEDALIS, V. R. V. RAMANAN and D. J. SKINNER, in "Thermal Analysis in Metallurgy," edited by R. D. Shull and A. Joshi (The Mineral, Metals & Materials Society, Pennsylvania, 1992) p. 279.

6. I. J. POLMEAR, M. J. COUPER and M. J. BANNISTER, *Mater. Forum.* **12** (1988) 54.
7. R. A. DUNLAP and K. DINI, *Can. J. Phys.* **63** (1985) 1267.
8. R. M. K. YOUNG and J. H. TWEED, *Mater. Sci. Eng A.* **A134** (1991) 1153.
9. M. AUDIER and P. GUYOT, *Phil. Mag. B.* **53**(1) (1986) L43.
10. R. D. FIELD, J. W. ZINDEL and H. L. FRASER, *Scripta Metall.* **20** (1991) 415.
11. M. CARRARD, M. GREMAUD and M. PIERANTONI, *Scripta Metall. Mater.* **25** (1991) 925.
12. L. A. BENDERSKY, A. J. MCALISTER and F. S. BIANCANIELLO, *Metall. Trans. A.* **19A** (1988) 2893.
13. A. FONTAINE, J. DIXMIER and A. GUINIER, *Fizika 2 Suppl.* **2** (1970) 23.1.
14. H. J. KOH, W. J. PARK and N. J. KIM, *Mater. Trans. JIM.* **39**(9) (1998) 982.
15. W. L. ZHOU, X. Z. LI and K. H. KUO, *Scripta Metall.* **23** (1989) 1571.
16. K. Y. WEN, Y. L. CHEN and K. H. KUO, *Metall. Trans. A.* **23A** (1992) 2437.